

1 Estimating soil moisture conditions for drought monitoring with 2 Random Forests and a simple soil moisture accounting scheme

3
4
5 Yves Trambly ^{1*}

6 Pere Quintana Seguí ²

7
8
9 1 HydroSciences Montpellier (University Montpellier, CNRS, IRD), France

10 2 Observatori de l'Ebre (OE), Ramon Llull University – CSIC, 43520 Roquetes, Spain

11
12
13 *Corresponding author : yves.trambly@ird.fr, 300 avenue du Pr. Emile Jeanbreaux,
14 34090, Montpellier, France. +33 4 67 14 33 59

15 16 **Abstract**

17
18 Soil moisture is a key variable for drought monitoring but soil moisture measurements
19 networks are very scarce. Land-surface models can provide a valuable alternative to
20 simulate soil moisture dynamics, but only a few countries have such modelling schemes
21 implemented for monitoring soil moisture at high spatial resolution. In this study, a soil
22 moisture accounting model (SMA) was regionalized over the Iberian Peninsula, taking as
23 a reference the soil moisture simulated by a high-resolution land surface model. To
24 estimate soil water holding capacity, the sole parameter required to run the SMA model,
25 two approaches were compared: the direct estimation from European soil maps using
26 pedotransfer functions, or an indirect estimation by a Machine Learning approach,
27 Random Forests, using as predictors altitude, temperature, precipitation, potential
28 evapotranspiration and land use. Results showed that the Random Forest model
29 estimates are more robust, especially for estimating low soil moisture levels.
30 Consequently, the proposed approach can provide an efficient way to simulate daily soil
31 moisture and therefore monitor soil moisture droughts, in contexts where high-resolution
32 soil maps are not available, as it relies on a set of covariates that can be reliably estimated
33 from global databases.

34
35
36
37
38 **Keywords:** soil moisture, droughts, random forests

1. Introduction

Soil moisture droughts have strong impacts on vegetation and agricultural production (Raymond et al., 2019; Trambly et al., 2020; Vicente-Serrano et al., 2014; Pena-Gallardo et al., 2019). There is a growing interest for simple indicators to monitor drought events at short timescales that could be related to impacts (Li et al., 2020; Noguera et al., 2021). In particular, soil moisture indicators could be more relevant than climatic ones to monitor potential impacts of droughts on agriculture and natural vegetation (Piedallu et al., 2013). Since actual soil moisture measurements remain very scarce, soil moisture simulated from land-surface models are an interesting proxy to develop simplified methodologies that could be applied on data-sparse regions. Land-surface models (LSM) are valuable tools for a fine scale monitoring of drought events; however, their implementation requires accurate forcing data and computational resources (Almendra-Martín et al., 2021; Quintana-Seguí et al., 2019; Barella-Ortiz and Quintana-Seguí, 2019). Global implementation also exists but with a coarser resolution and driven by reanalysis data (Rodell et al., 2004; Muñoz Sabater, 2020) that may not be adequate for local-scale applications. Only very few countries have land-surface schemes implemented at the national level to monitor droughts (Habets et al., 2008).

Remote Sensing is another option which allows monitoring soil moisture (Dorigo et al., 2017; Brocca et al., 2019). Microwave sensors allow monitoring of surface soil moisture (first 5 cm for L-band based products, skin for C-band based products), without the interference of clouds. However, surface soil moisture is not enough for most applications, which require root zone soil moisture, which is the water resource in the soil available to plants. Furthermore, passive L-band products, such as SMOS (Martínez-Fernández et al., 2016) or SMAP (Mishra et al., 2017), have a low resolution and active C-band products, such as Sentinel 1 (Bauer-Marschallinger et al., 2019), which have higher resolution, suffer from higher noise and are more sensitive to vegetation. Thus, even though remote sensing is very useful, it still has problems to be surmounted. The resolution of passive L-band products can be increased using optical data (NDVI, LST), by means of downscaling algorithms (Merlin et al., 2013; Fang et al., 2021), but then the resulting product is sensitive to cloud cover. Also, some progress has been made in deriving root zone soil moisture from surface soil moisture estimations using an exponential filter (Stefan et al., 2021) calibrated using the SURFEX LSM (Masson et al., 2013), but these products are in early stages and are not operational yet.

Simplified methodologies to estimate and monitor the status of soil moisture, are needed in contexts where LSM data is not available and where remote sensing products fall short, such as areas and time periods with dense vegetation, or high soil roughness which may affect their accuracy (Escorihuela and Quintana-Seguí, 2016). Different modelling

81 approaches have been proposed, either with conceptual soil moisture accounting models
82 or computational variants of the antecedent precipitation index (Willgoose and Perera,
83 2001; Javelle et al., 2010; Brocca et al., 2014; Zhao et al., 2019; Li et al., 2020). The
84 general availability of spatial estimates of soil moisture content would help introduce soil
85 moisture in drought monitoring systems, improving their scope and usefulness.
86 Furthermore, this would also facilitate the creation of long-term reanalysis, based on
87 meteorological forcing data, and future climate change studies, without the need of
88 running LSM models. However, to apply this type of models at regional or national scale,
89 there is a need to estimate their parameters over the area of interest. For that purpose,
90 regionalization methods have been employed in hydrology for decades to estimate the
91 parameters of hydrological models in ungauged basins (Blöschl and Sivapalan, 1995; He
92 et al., 2011; Hrachowitz et al., 2013). Several methods exist, based either on catchment
93 similarity or the direct estimation of model parameters using regression techniques with
94 physiographic attributes. For soil moisture modelling, up to now only very few studies
95 have considered these approaches to apply soil moisture accounting models at ungauged
96 locations (Grillakis et al., 2021) or estimate root zone soil moisture using machine learning
97 methods (Carranza et al., 2021).

98
99 The goal of the present study is to regionalize a simple soil moisture accounting (SMA)
100 scheme that could be used to monitor soil moisture droughts. The SMA model considered
101 in the present study requires a single parameter, the maximum soil water holding
102 capacity. Two different approaches are compared to estimate this parameter regionally:
103 the direct estimation with soil maps or with a machine learning technique, namely
104 Random Forests.

105

106 **2. Study area and Data**

107

108 The study area of this work is the Iberian Peninsula, which is located between the
109 Mediterranean Sea and the Atlantic Ocean and thus is influenced by both synoptic scale
110 systems, that often come from the Atlantic side, and mesoscale heavy precipitation
111 events, that often come from the Mediterranean side. The Iberian Peninsula presents a
112 marked relief, with a large and high central plateau and different mountain ranges, which
113 heavily influence the spatial patterns of precipitation, enhancing it windward and
114 decreasing it leeward, generating areas of high precipitation on the west, north-west and
115 north, and very dry areas on the central plains and, specially, on the South-east, as a
116 consequence the Iberian Peninsula has a heterogeneous distribution of average annual
117 rainfall, with values ranging from 2000 mm/y to less than 100 mm/y. All this has a strong
118 influence on the spatial and temporal variability of soil moisture and soil moisture regimes,
119 having wet regimes on the west and north, where the soil is hardly stressed and, and
120 semi-arid areas elsewhere, with a wet (energy limited) and a dry (water limited) season,

121 with a dry down that might be interrupted by convective events. All this makes the
122 modelling of soil moisture in Iberian a rather challenging task.

123
124 Daily precipitation, temperature and potential evapotranspiration (PET) were retrieved
125 from the SAFRAN-Spain database (Quintana-Seguí et al., 2017). SAFRAN (Durand et
126 al., 1993) is a meteorological reanalysis that produces gridded datasets by combining the
127 outputs of a meteorological model and all available observations using an optimal
128 interpolation algorithm. It has been implemented over France (Quintana-Seguí et al.,
129 2008) and recently over the Iberian Peninsula (Quintana-Seguí et al., 2017) with a
130 5kmx5km spatial resolution. The SAFRAN dataset used in this study not only includes
131 observations from the Spanish part of the Iberian Peninsula, it has also ingested data
132 from Portugal. The SURFEX LSM (Masson et al., 2013) has been run using SAFRAN-
133 Spain as the meteorological forcing dataset and on the same grid, as it was done in
134 Quintana-Seguí et al., (2019). SURFEX uses the ECOCLIMAP2 (Faroux et al., 2013)
135 physiographic database and it uses the ISBA (Interaction Sol-Biosphère-Atmosphère)
136 scheme (Noilhan and Mahfouf, 1996) for natural surfaces. ISBA has different options; we
137 have used ISBA-DIF, the multi-layer diffusion version (Boone 2000; Habets et al. 2003).
138 From this simulation, we have extracted the soil moisture of the first 60 cm of the soil, by
139 performing the weighted average of the soil layers that fall within this range. This
140 simulated soil moisture over the Iberian Peninsula is considered herein as the observed
141 reference, in the absence of dense monitoring networks of soil moisture (Martínez-
142 Fernández et al., 2016). From the ECOCLIMAP2 database, elevation and land cover data
143 have also been retrieved and aggregated in the following nine categories: water, bare,
144 ice/snow, urban, forest, grass, dry crops, irrigated crops, wetlands.

145
146 We also use the European Soil database (ESDB) produced by the European Soil Data
147 Centre (Panagos et al., 2012). The ESDB contains information on soil characteristics,
148 including soil depth and texture for topsoil (0-30cm) and subsoil (30-70cm) layers at a
149 grid resolution of 1 km. The total available water content (TAWC) is a volumetric
150 parameter describing the water content between field capacity and permanent wilting
151 point, as a function of available water content, presence of coarse fragments and depth
152 (Reynolds et al., 2000). In ESDB, water content at field capacity and permanent wilting
153 point were determined following the equation from (van Genuchten, 1980) to estimate the
154 soil water retention curve (Hiederer, 2013). The parameters of the equation are provided
155 by a pedotransfer function (Wösten et al., 1999) for volumetric soil water content
156 computed from the soil water retention curve. The pedotransfer function uses soil texture,
157 organic carbon content and bulk density to determine the parameters of the soil water
158 retention curve (Hiederer, 2013).

159
160 **3. Methods**

161

162 3.1 Soil moisture accounting model

163

164 The soil moisture model considered here has been previously applied in several studies
165 for applications related to soil moisture monitoring (Anctil et al., 2004; Javelle et al., 2010;
166 Tramblay et al., 2012, 2014), it consists in the SMA part of the GR4J model (Perrin et al.,
167 2003), driven by precipitation and PET, that represents a conceptual formulation of the
168 impact of precipitation and PET on soil water balance, using a soil reservoir of fixed depth,
169 A. This parameter represents the maximum capacity of that reservoir, that can be
170 assumed to be equivalent to the soil water holding capacity (Perrin et al., 2003, Javelle
171 et al., 2010, Tramblay et al., 2014). The soil reservoir has either a net outflow when PET
172 exceed rainfall:

173

174 If $P_t \leq PET_t$

$$175 \quad S^* = S_{t-1} - \frac{S_{t-1}(2A - S_{t-1}) \tanh\left(\frac{PET_t - P_t}{A}\right)}{A + (A - S_{t-1}) \tanh\left(\frac{PET_t - P_t}{A}\right)} \quad (1)$$

176

177 Or net inflow in all the other cases:

178

179 If $P_t \leq PET_t$

$$180 \quad S^* = S_{t-1} + \frac{(A^2 - S_{t-1}^2) \tanh\left(\frac{P_t - PET_t}{A}\right)}{(A + S_{t-1}) \tanh\left(\frac{P_t - PET_t}{A}\right)} \quad (2)$$

181

182 Where S^* can never exceed the maximum reservoir capacity. Finally, the outflow from
183 the storage reservoir due to percolation is taken into account using:

184

$$185 \quad S_t = S^* \left[1 + \left(\frac{4S^*}{9A} \right)^4 \right]^{-\frac{1}{4}} \quad (3)$$

186

187 The level of the soil reservoir is given by S/A , ranging between 0 and 1, which provides a
188 soil wetness index (SWI) for the catchment. The outputs of SURFEX soil moisture are
189 first normalized with the maximum and minimum values, to obtain a SWI consistent with
190 the SMA model output. Then, the SMA model parameter A is calibrated using this
191 normalized SURFEX soil moisture as a reference. The SMA model is calibrated for each
192 grid cell independently using soil moisture simulated with SURFEX covering the full
193 Iberian Peninsula domain. The Nelder-Mead simplex algorithm is used for the calibration
194 with the Nash efficiency criterion. To regionally estimate the values of A , two different
195 methods are compared: the direct estimation of A with TAWC from ESDB soil maps or its
196 indirect estimation with machine learning methods, namely Random Forests using
197 5kmx5km grid physiographic and climatic properties.

198

199 **3.2 Regionalization with soil maps**

200

201 The first approach consists in using the total available water content from the ESDB
202 database to estimate the A parameter for each grid cell. In the present work, the TAWC
203 of subsoil and topsoil layers have been added and averaged at the scale of 5km x 5km,
204 matching the spatial resolution of the SAFRAN grid. Then, these estimates have been
205 used to set the A parameter of the SMA model. Thus, this regionalization approach is
206 based on the a priori estimation of the A parameter from soil maps solely.

207

208 **3.3 Regionalization with Random forests**

209

210 Random Forests (Breiman, 2001) belong to the class of Machine Learning techniques.
211 RF are based on a bootstrap aggregation (Breiman, 1996) of Classification and
212 Regression Trees (Breiman et al., 2017). It generates a bootstrap sample from the original
213 data and trains a tree model using this sample. The procedure is repeated many times
214 and the bagging's prediction is the average of the predictions. Among the many
215 advantages of RF, they are fast, non-parametric, robust to noise in the predictor variables,
216 able to capture nonlinear dependencies between predictors and dependent variables and
217 they can simultaneously incorporate continuous and categorical variables (Tyrallis et al.,
218 2019). The drawbacks are they are complex to interpret and they cannot extrapolate
219 outside the training range. Given their advantages, this algorithm is particularly suited for
220 the estimation of spatial variables such as soil properties (Booker and Woods, 2014;
221 Hengl et al., 2018; Gagkas and Lilly, 2019; Stein et al., 2021). In the present work, a RF
222 model is generated to estimate the values of the A parameter of the SMA model,
223 representing soil water holding capacity, with the properties of the 5x5km grid cells namely
224 altitude, land cover, mean annual precipitation, temperature and PET, using Random Forests.

225

226 To estimate the reliability of the method, the 5km x 5km grid cells covering the Iberian
227 Peninsula have been split randomly into a training sample containing 70% of the cells
228 (15636 data points) and a testing sample with the 30% remaining cells (6701 data points).
229 The random selection of the training and testing sets have been performed using a Latin
230 Hypercube Sampling (McKay et al., 1979) to ensure a homogeneous sampling over the
231 Iberian Peninsula. Given that the RF trees cannot be interpreted directly, as for example
232 the weights in a linear regression, we additionally implemented an out-of-bag predictor
233 importance estimation by permutation (Loh and Shih, 1997), to measure how influential
234 the predictor variables in the model are at predicting the response. The influence of a
235 predictor increases with the value of this measure. If a predictor is influential in prediction,
236 then permuting its values should affect the model error. If a predictor is not influential,
237 then permuting its values should have little to no effect on the model error.

238

239 **3.3 Validation on the ability to detect dry soil moisture conditions**

240

241 To compare the efficiency of the two methods compared to estimate the A parameter of
242 the SMA model, the SMA model was run using the two methods and all daily values of
243 soil moisture below the 10th percentile were extracted, corresponding to dry soil
244 conditions. Only the grid cells in the testing sample were considered for this validation.
245 We computed different verification scores to assess the relative efficiency of the two
246 methods to reproduce daily soil moisture below the 10th percentile using the ISBA
247 simulated soil moisture as a benchmark; the Probability of Detection (POD), the False
248 Alarm Ratio (FAR) and the Heidke Skill Score (HSS) summarizing the global efficiency to
249 detect dry periods (Jolliffe and Stephenson, 2011). These scores are based on the
250 contingency table between forecasts (or simulated values in the case of the present
251 study) and observations (Table 1).

252

253 POD is the probability of detection (equation 1), FAR is the number of false alarms per
254 the total number of warnings or alarms (equation 2) and HSS is a skill score ranging from
255 $-\infty$ to 1 (equation 3), for categorical forecasts where the proportion of correct measure is
256 scaled with the reference value from correct forecasts due to chance.

257

$$258 \text{ } POD = a / (a + c) \quad (4)$$

259

$$260 \text{ } FAR = b / (a + b) \quad (5)$$

261

$$262 \text{ } HSS = 2 (ad - bc) / (a + b)(b + d) + (a + c)(c + d) \quad (6)$$

263

264

265 **4. Results**

266

267 **4.1 Calibration of the SMA model**

268

269 The calibration results of the SMA model against SURFEX soil moisture provide very
270 good model performance, with a mean Nash coefficient equal to 0.94, indicating its ability
271 to reproduce the soil moisture dynamics as simulated by SURFEX. Nash values below
272 0.5 are found for 1.21 % of grid cells (n= 273), only for areas located in the mountainous
273 range affected by snow processes, above 1500 m.a.s.l. (Figure 1). This outcome is
274 expected, since the SMA model does not include a snow-module it cannot reproduce
275 snow dynamics in these areas. However, high-elevation areas with seasonal snow cover
276 are not the area's most at risk of soil moisture droughts for agricultural activities in Spain.
277 The calibrated values of the A parameter of the SMA model ranges from 60 to 250 mm,
278 depending on the location (Figure 3). There is no significant correlation between A and
279 mean annual precipitation or the aridity index (P/PET). This highlights the interplays
280 between soil properties and climate to explain the spatial variability on soil water holding
281 capacity.

282

283 **4.2 Regional estimation of the A parameter**

284

285 The values of the calibrated A parameter are related to the properties of the 5x5km grid
286 cells using Random Forests. First, an out-of-bag predictor importance estimation by
287 permutation is applied to compute the overall performance of RF and estimate the relative
288 influence of each predictor. When using the A out-of-bag estimates to run the SMA model,
289 the loss of performance is very small, the decrease in Nash values in validation is on
290 average equal -0.0019 (with a maximum decrease of -0.04). This is due to the small
291 sensitivity of the SMA model to the value of A, given that the error in the estimation of A
292 is in the range of 10 mm (RMSE = 13.18 mm). This type of validation mimics the case
293 when the estimation at one single location is required, yet since all the remaining points
294 are used for the estimation, it makes the approach in that case very robust. The relative
295 importance for each predictor is plotted on Figure 3, indicating that precipitation and
296 potential evapotranspiration are two most important predictors, followed by altitude. On
297 the contrary, the land cover attributes for each grid cell are the least important predictors,
298 and removing them from the RF model does not significantly change the results. This
299 shows the relative importance of climatic variables in the spatial variability of soil moisture
300 holding capacity.

301

302 To estimate the robustness of the method, we applied a split-sample validation into a
303 testing and a training sample. The results are presented for the testing set (Figure 4). The
304 performance in terms of Nash for the SMA model with A estimated by Random Forests
305 or soil map is very similar, with mean Nash equal to 0.86 (median = 0.89) with RF and

306 0.81 (median = 0.85) with soil maps. The Nash values in validation (testing set) are low,
307 or even negative, only for mountainous ranges, as expected. Overall, the spatial patterns
308 of the Nash coefficients obtained with RF or ESDB are very similar too. There are no
309 significant relationships between model efficiency and the aridity index or the presence
310 of irrigated areas, as identified in the ECOCLIMAP2 land cover database.

311

312 **4.3 Estimation of dry soil conditions**

313

314 A further validation is made for daily soil moisture below the 10th percentile corresponding
315 to dry soil conditions. We computed the Probability of Detection (POD), the False Alarm
316 Ratio (FAR) and the Heidke Skill Score (HSS) summarizing the global efficiency to detect
317 dry periods. For both approaches to estimate A, the mean POD is very high, close to
318 97%, while the FAR is close to 3%. But these average results hide some discrepancy in
319 the different regions (Figure 5): the efficiency is the highest for the North-Western region,
320 the wettest areas of Spain, with the most important increase of HSS and POD, associated
321 with a decrease in FAR, using Random forests, while in the South and Central parts of
322 Spain the performance is lower on average and very similar with the two regionalization
323 approaches. For the wettest parts of the Iberian Peninsula, the POD remains higher than
324 94% and the FAR lower than 6% and it is the region where the main improvements with
325 RF are observed. As shown in Figure 5, the results with Random forests mostly follow the
326 climate conditions, with improved estimations in the wettest regions of North and
327 Northwestern part of Spain. For the estimation with EU soil maps, the results seem related
328 to soil depth and to a lesser extent, land cover. Indeed, higher scores are found in regions
329 with shallow soils, such as those of plutonic (Galician region, western parts of the
330 Extremaduran mountainous ranges, Douro basin) or metamorphic origins (western
331 Cantabric range, north Iberian range, eastern-central regions and Sierra Morena in
332 Andalusia) and also sedimentary regions with shallow limestones (eastern Cantabric
333 mountains, Basque region, Southern Iberian range). On the opposite, lower scores are
334 found in regions with the deepest soils (Guadalquivir floodplains, Mid- Tagus River, upper
335 Duero, piedmonts of Cantabric in Leon and Palencia, most of Middle Navarra). With the
336 exception of regions such as Bizcaya or coastal Portugal, with a dense forest cover
337 (mostly *Pinus radiata* or *pinaster*) where soil depth is probably overestimated. On
338 average, the RF estimation method outperforms the approach based on ESDB (Figure
339 7), with more stable results in terms of HSS since all values obtained with RF are above
340 0.4 while with ESDB for the grid cells the HSS scores drops to values close to zero.

341

342 **5. Summary and conclusions**

343

344 In this study, a simple model allowing the monitoring of soil moisture conditions was
345 regionalized over the entire Iberian Peninsula, taking as a reference the soil moisture

346 simulated by a high-resolution land surface model. Two different regionalization methods
347 have been compared, either the direct estimation of soil water holding capacity from
348 European soil maps or by Random Forests, using covariates such as altitude,
349 temperature, precipitation, potential evapotranspiration and land cover. Results have
350 shown that the estimation by Random Forest is more robust notably to estimate low soil
351 moisture levels. Despite similar average performance between the two methods, the use
352 of soil maps to set the water holding capacity reveals less stable results in some cases,
353 most probably related to the uncertainties in the pedo-transfer functions used. While these
354 pedo-transfer functions are process-based predictive functions of certain soil properties,
355 Random Forest are not based on physical processes and are tailored to provide the best
356 estimates in a statistical sense. Therefore, they provide a valuable alternative in contexts
357 where high-resolution soil maps are not available since they rely on a set of covariates
358 that can be reliably estimated from global databases, such as satellite or reanalysis
359 products (Funk et al., 2015; Hersbach et al., 2020; Muñoz Sabater, 2020).

360
361 It should be noted that the results presented herein are highly dependent on the quality
362 of land surface simulations, in the absence of dense monitoring networks of in situ soil
363 moisture data, thus these results suffer from the same limitations as LSMs, notably, the
364 lack of human processes (irrigation). However, new remote sensing irrigation estimates
365 are being developed (Massari et al., 2021), as a consequence, once the RF model is
366 trained, irrigation estimations could be added to the precipitation forcing data in order to
367 include the human impacts on soil moisture estimations. The results show that this
368 approach allows us to cheaply extend the value of high resolution LSM simulations to
369 areas where no LSM is implemented (ie. north Africa), as long as the climate conditions
370 belong to the range of values used to train the model, mostly in terms of precipitation and
371 potential evapotranspiration ranges. Thus, the model train over the Iberian Peninsula
372 could be applied to other similar areas such as North Africa, Italy or Greece. As a
373 perspective, other simulations from countries where high resolution LSM simulations are
374 available, such as France or the USA, could be added to the database in order to expand
375 the coverage over different physiographic and climate contexts (Ma et al., 2021).
376 Consequently, the benefits of LSM simulations of soil moisture could be expanded to
377 other areas, provided that suitable forcing datasets are available. Furthermore, if public
378 meteorological and hydrological organizations were to create soil moisture observation
379 networks, cleverly designed to cover the most relevant climates of their countries, this
380 approach could be used to train the model using these observations and then regionalize
381 the results to the rest of the territory, thus, converting an *in-situ* observation dataset into
382 a gridded dataset with a much greater spatial coverage.

383
384

385 **Acknowledgements**

386 This work is a contribution to the HyMeX programme through the HUMID (CGL2017-
387 85687-R, AEI/FEDER, UE) and ANR HILIAISE projects. We thank Jaime Gaona (Instituto
388 de Investigación en agrobiotecnología CIALE, Universidad de Salamanca , Villamayor,
389 Salamanca, Spain) for his comments on some aspects of the manuscript, and two anonymous
390 reviewers for their suggestions to improve the manuscript.

391

392

393 **References**

394

395 Almendra-Martín, L., Martínez-Fernández, J., González-Zamora, Á., Benito-Verdugo, P., and
396 Herrero-Jiménez, C. M.: Agricultural Drought Trends on the Iberian Peninsula: An Analysis
397 Using Modeled and Reanalysis Soil Moisture Products, *Atmosphere*, 12, 236,
398 <https://doi.org/10.3390/atmos12020236>, 2021.

399

400 Anctil, F., Michel, C., Perrin, C., and Andréassian, V.: A soil moisture index as an auxiliary ANN
401 input for stream flow forecasting, *Journal of Hydrology*, 286, 155–167,
402 <https://doi.org/10.1016/j.jhydrol.2003.09.006>, 2004.

403

404 Barella-Ortiz, A. and Quintana-Seguí, P.: Evaluation of drought representation and propagation
405 in regional climate model simulations across Spain, *Hydrol. Earth Syst. Sci.*, 23, 5111–5131,
406 <https://doi.org/10.5194/hess-23-5111-2019>, 2019.

407

408 Bauer-Marschallinger, B., Freeman, V., Cao, S., Paulik, C., Schaufler, S., Stachl, T., Modanesi,
409 S., Massari, C., Ciabatta, L., Brocca, L., and Wagner, W.: Toward Global Soil Moisture
410 Monitoring With Sentinel-1: Harnessing Assets and Overcoming Obstacles, *IEEE Trans.*
411 *Geosci. Remote Sensing*, 57, 520–539, <https://doi.org/10.1109/TGRS.2018.2858004>, 2019.

412

413 Blöschl, G. and Sivapalan, M.: Scale issues in hydrological modelling: A review, *Hydrol.*
414 *Process.*, 9, 251–290, <https://doi.org/10.1002/hyp.3360090305>, 1995.

415

416 Booker, D. J. and Woods, R. A.: Comparing and combining physically-based and empirically-
417 based approaches for estimating the hydrology of ungauged catchments, *Journal of Hydrology*,
418 508, 227–239, <https://doi.org/10.1016/j.jhydrol.2013.11.007>, 2014.

419

420 Boone, A., :Modélisation des processus hydrologiques dans le schéma de surface ISBA:
421 Inclusion d'un réservoir hydrologique, du gel et modélisation de la neige. PhD thesis, Université
422 Paul Sabatier (Toulouse III), http://www.cnrm.meteo.fr/IMG/pdf/boone_thesis_2000.pdf, 2000.

423

424 Breiman, L.: Bagging predictors, *Mach Learn*, 24, 123–140,
425 <https://doi.org/10.1007/BF00058655>, 1996.

426

427 Breiman, L.: Random Forests, 45, 5–32, <https://doi.org/10.1023/A:1010933404324>, 2001.

428

429 Breiman, L., Friedman, J. H., Olshen, R. A., and Stone, C. J.: *Classification And Regression*
430 *Trees*, 1st ed., Routledge, <https://doi.org/10.1201/9781315139470>, 2017.

431

432 Brocca, L., Camici, S., Melone, F., Moramarco, T., Martínez-Fernández, J., Didon-Lescot, J.-F.,
433 and Morbidelli, R.: Improving the representation of soil moisture by using a semi-analytical

434 infiltration model, *Hydrol. Process.*, 28, 2103–2115, <https://doi.org/10.1002/hyp.9766>, 2014.

435

436 Brocca, L., Filippucci, P., Hahn, S., Ciabatta, L., Massari, C., Camici, S., Schüller, L., Bojkov, B.,
437 and Wagner, W.: SM2RAIN–ASCAT (2007–2018): global daily satellite rainfall data from
438 ASCAT soil moisture observations, *Earth Syst. Sci. Data*, 11, 1583–1601,
439 <https://doi.org/10.5194/essd-11-1583-2019>, 2019.

440

441 Carranza, C., Nolet, C., Peziz, M., and van der Ploeg, M.: Root zone soil moisture estimation
442 with Random Forest, *Journal of Hydrology*, 593, 125840,
443 <https://doi.org/10.1016/j.jhydrol.2020.125840>, 2021.

444

445 Dorigo, W., Wagner, W., Albergel, C., Albrecht, F., Balsamo, G., Brocca, L., Chung, D., Ertl, M.,
446 Forkel, M., Gruber, A., Haas, E., Hamer, P. D., Hirschi, M., Ikonen, J., de Jeu, R., Kidd, R.,
447 Lahoz, W., Liu, Y. Y., Miralles, D., Mistelbauer, T., Nicolai-Shaw, N., Parinussa, R., Pratola, C.,
448 Reimer, C., van der Schalie, R., Seneviratne, S. I., Smolander, T., and Lecomte, P.: ESA CCI
449 Soil Moisture for improved Earth system understanding: State-of-the art and future directions,
450 *Remote Sensing of Environment*, 203, 185–215, <https://doi.org/10.1016/j.rse.2017.07.001>,
451 2017.

452

453 Durand, Y., Brun, E., Merindol, L., Guyomarc’h, G., Lesaffre, B., and Martin, E.: A
454 meteorological estimation of relevant parameters for snow models, *A. Glaciology.*, 18, 65–71,
455 <https://doi.org/10.1017/S0260305500011277>, 1993.

456

457 Escorihuela, M. J. and Quintana-Seguí, P.: Comparison of remote sensing and simulated soil
458 moisture datasets in Mediterranean landscapes, *Remote Sensing of Environment*, 180, 99–114,
459 <https://doi.org/10.1016/j.rse.2016.02.046>, 2016.

460

461 Fang, B., Kansara, P., Dandridge, C., and Lakshmi, V.: Drought monitoring using high spatial
462 resolution soil moisture data over Australia in 2015–2019, *Journal of Hydrology*, 594, 125960,
463 <https://doi.org/10.1016/j.jhydrol.2021.125960>, 2021.

464

465 Faroux, S., Kaptué Tchuenté, A. T., Roujean, J.-L., Masson, V., Martin, E., and Le Moigne, P.:
466 ECOCLIMAP-II/Europe: a twofold database of ecosystems and surface parameters at 1 km
467 resolution based on satellite information for use in land surface, meteorological and climate
468 models, *Geosci. Model Dev.*, 6, 563–582, <https://doi.org/10.5194/gmd-6-563-2013>, 2013.

469

470 Funk, C., Peterson, P., Landsfeld, M., Pedreros, D., Verdin, J., Shukla, S., Husak, G., Rowland,
471 J., Harrison, L., Hoell, A., and Michaelsen, J.: The climate hazards infrared precipitation with
472 stations—a new environmental record for monitoring extremes, *Sci Data*, 2, 150066,
473 <https://doi.org/10.1038/sdata.2015.66>, 2015.

474

475 Gagkas, Z. and Lilly, A.: Downscaling soil hydrological mapping used to predict catchment
476 hydrological response with random forests, *Geoderma*, 341, 216–235,
477 <https://doi.org/10.1016/j.geoderma.2019.01.048>, 2019.

478

479 van Genuchten, M. Th.: A Closed-form Equation for Predicting the Hydraulic Conductivity of
480 Unsaturated Soils, *Soil Science Society of America Journal*, 44, 892–898,
481 <https://doi.org/10.2136/sssaj1980.03615995004400050002x>, 1980.

482

483 Grillakis, M. G., Koutroulis, A. G., Alexakis, D. D., Polykretis, C., and Daliakopoulos, I. N.:

484 Regionalizing Root-Zone Soil Moisture Estimates From ESA CCI Soil Water Index Using
485 Machine Learning and Information on Soil, Vegetation, and Climate, *Water Res*, 57,
486 <https://doi.org/10.1029/2020WR029249>, 2021.
487
488 Habets F., Boone A., and Noilhan J.: Simulation of a Scandinavian basin using the diffusion
489 transfer version of ISBA. *Glob Planet Chang* 38(1-2):137–149, 2003.
490
491 Habets, F., Boone, A., Champeaux, J. L., Etchevers, P., Franchistéguy, L., Leblois, E., Ledoux,
492 E., Le Moigne, P., Martin, E., Morel, S., Noilhan, J., Quintana Seguí, P., Rousset-Regimbeau,
493 F., and Viennot, P.: The SAFRAN-ISBA-MODCOU hydrometeorological model applied over
494 France, *J. Geophys. Res.*, 113, D06113, <https://doi.org/10.1029/2007JD008548>, 2008.
495
496 He, Y., Bárdossy, A., and Zehe, E.: A review of regionalisation for continuous streamflow
497 simulation, *Hydrol. Earth Syst. Sci.*, 15, 3539–3553, <https://doi.org/10.5194/hess-15-3539-2011>,
498 2011.
499
500 Hengl, T., Nussbaum, M., Wright, M. N., Heuvelink, G. B. M., and Gräler, B.: Random forest as
501 a generic framework for predictive modeling of spatial and spatio-temporal variables, 6, e5518,
502 <https://doi.org/10.7717/peerj.5518>, 2018.
503
504 Hersbach, H., Bell, B., Berrisford, P., Hirahara, S., Horányi, A., Muñoz-Sabater, J., Nicolas, J.,
505 Peubey, C., Radu, R., Schepers, D., Simmons, A., Soci, C., Abdalla, S., Abellan, X., Balsamo,
506 G., Bechtold, P., Biavati, G., Bidlot, J., Bonavita, M., Chiara, G., Dahlgren, P., Dee, D.,
507 Diamantakis, M., Dragani, R., Flemming, J., Forbes, R., Fuentes, M., Geer, A., Haimberger, L.,
508 Healy, S., Hogan, R. J., Hólm, E., Janisková, M., Keeley, S., Laloyaux, P., Lopez, P., Lupu, C.,
509 Radnoti, G., Rosnay, P., Rozum, I., Vamborg, F., Villaume, S., and Thépaut, J.: The ERA5
510 global reanalysis, *Q.J.R. Meteorol. Soc.*, 146, 1999–2049, <https://doi.org/10.1002/qj.3803>, 2020.
511
512 Hiederer, R.: Mapping soil properties for Europe: spatial representation of soil database
513 attributes., Publications Office, LU, 2013.
514
515 Hrachowitz, M., Savenije, H. H. G., Blöschl, G., McDonnell, J. J., Sivapalan, M., Pomeroy, J. W.,
516 Arheimer, B., Blume, T., Clark, M. P., Ehret, U., Fenicia, F., Freer, J. E., Gelfan, A., Gupta, H.
517 V., Hughes, D. A., Hut, R. W., Montanari, A., Pande, S., Tetzlaff, D., Troch, P. A., Uhlenbrook,
518 S., Wagener, T., Winsemius, H. C., Woods, R. A., Zehe, E., and Cudennec, C.: A decade of
519 Predictions in Ungauged Basins (PUB)—a review, *Hydrological Sciences Journal*, 58, 1198–
520 1255, <https://doi.org/10.1080/02626667.2013.803183>, 2013.
521
522 Javelle, P., Fouchier, C., Arnaud, P., and Lavabre, J.: Flash flood warning at ungauged
523 locations using radar rainfall and antecedent soil moisture estimations, *Journal of Hydrology*,
524 394, 267–274, <https://doi.org/10.1016/j.jhydrol.2010.03.032>, 2010.
525
526 Jolliffe, I. T. and Stephenson, D. B. (Eds.): *Forecast Verification: A Practitioner’s Guide in*
527 *Atmospheric Science*, John Wiley & Sons, Ltd, Chichester, UK,
528 <https://doi.org/10.1002/9781119960003>, 2011.
529
530 Li, J., Wang, Z., Wu, X., Xu, C.-Y., Guo, S., and Chen, X.: Toward Monitoring Short-Term
531 Droughts Using a Novel Daily Scale, Standardized Antecedent Precipitation Evapotranspiration
532 Index, 21, 891–908, <https://doi.org/10.1175/JHM-D-19-0298.1>, 2020.
533

534 Loh, W. Y. and Shih, Y. S.: Split Selection Methods for Classification Trees, 7, 815–840, 1997.
535 Martínez-Fernández, J., González-Zamora, A., Sánchez, N., and Gumuzzio, A.: A soil water
536 based index as a suitable agricultural drought indicator, *Journal of Hydrology*, 522, 265–273,
537 <https://doi.org/10.1016/j.jhydrol.2014.12.051>, 2015.
538
539 Martínez-Fernández, J., González-Zamora, A., Sánchez, N., Gumuzzio, A., and Herrero-
540 Jiménez, C. M.: Satellite soil moisture for agricultural drought monitoring: Assessment of the
541 SMOS derived Soil Water Deficit Index, *Remote Sensing of Environment*, 177, 277–286,
542 <https://doi.org/10.1016/j.rse.2016.02.064>, 2016.
543
544 Ma, K., Feng, D., Lawson, K., Tsai, W.-P., Liang, C., Huang, X., Sharma, A., Shen, C.:
545 Transferring hydrologic data across continents – leveraging data-rich regions to improve
546 hydrologic prediction in data-sparse regions. *Water Resources Research*, 57, e2020WR028600.
547 <https://doi.org/10.1029/2020WR028600>, 2021.
548
549 Massari, C., Modanesi, S., Dari, J., Gruber, A., De Lannoy, G. J. M., Giroto, M., Quintana-
550 Seguí, P., Le Page, M., Jarlan, L., Zribi, M., Ouaadi, N., Vreugdenhil, M., Zappa, L., Dorigo, W.,
551 Wagner, W., Brombacher, J., Pelgrum, H., Jaquot, P., Freeman, V., Volden, E., Fernandez
552 Prieto, D., Tarpanelli, A., Barbetta, S., and Brocca, L.: A Review of Irrigation Information
553 Retrievals from Space and Their Utility for Users, *Remote Sensing*, 13, 4112,
554 <https://doi.org/10.3390/rs13204112>, 2021.
555
556 Masson, V., Le Moigne, P., Martin, E., Faroux, S., Alias, A., Alkama, R., Belamari, S., Barbu, A.,
557 Boone, A., Bouyssel, F., Brousseau, P., Brun, E., Calvet, J. C., Carrer, D., Decharme, B., Delire,
558 C., Donier, S., Essauini, K., Gibelin, A. L., ... Voldoire, A. (2013). The SURFEXv7.2 land and
559 ocean surface platform for coupled or offline simulation of earth surface variables and fluxes.
560 *Geoscientific Model Development*, 6(4), 929–960. <https://doi.org/10.5194/gmd-6-929-2013>
561
562 McKay, M. D., Beckman, R. J., and Conover, W. J.: Comparison of Three Methods for Selecting
563 Values of Input Variables in the Analysis of Output from a Computer Code, *Technometrics*, 21,
564 239–245, <https://doi.org/10.1080/00401706.1979.10489755>, 1979.
565
566 Merlin, O., Escorihuela, M. J., Mayoral, M. A., Hagolle, O., Al Bitar, A., and Kerr, Y.: Self-
567 calibrated evaporation-based disaggregation of SMOS soil moisture: An evaluation study at 3
568 km and 100 m resolution in Catalunya, Spain, *Remote Sensing of Environment*, 130, 25–38,
569 <https://doi.org/10.1016/j.rse.2012.11.008>, 2013.
570
571 Mishra, A., Vu, T., Veettil, A. V., and Entekhabi, D.: Drought monitoring with soil moisture active
572 passive (SMAP) measurements, *Journal of Hydrology*, 552, 620–632,
573 <https://doi.org/10.1016/j.jhydrol.2017.07.033>, 2017.
574
575 Muñoz Sabater, J.: ERA5-Land hourly data from 1981 to present. Copernicus Climate Change
576 Service (C3S) Climate Data Store (CDS), 10.24381/cds.e2161bac, 2020.
577
578 Noguera, I., Domínguez-Castro, F., and Vicente-Serrano, S. M.: Flash Drought Response to
579 Precipitation and Atmospheric Evaporative Demand in Spain, *Atmosphere*, 12, 165,
580 <https://doi.org/10.3390/atmos12020165>, 2021.
581
582 Noilhan, J. and Mahfouf, J.-F.: The ISBA land surface parameterisation scheme, *Global and*
583 *Planetary Change*, 13, 145–159, [https://doi.org/10.1016/0921-8181\(95\)00043-7](https://doi.org/10.1016/0921-8181(95)00043-7), 1996.

584
585 Panagos, P., Van Liedekerke, M., Jones, A., and Montanarella, L.: European Soil Data Centre:
586 Response to European policy support and public data requirements, *Land Use Policy*, 29, 329–
587 338, <https://doi.org/10.1016/j.landusepol.2011.07.003>, 2012.
588
589 Pena-Gallardo, M., Vicente-Serrano, S. M., Domínguez-Castro, F., and Beguería, S.: The
590 impact of drought on the productivity of two rainfed crops in Spain, *Nat. Hazards Earth Syst.*
591 *Sci.*, 19, 1215–1234, <https://doi.org/10.5194/nhess-19-1215-2019>, 2019.
592
593 Perrin, C., Michel, C., and Andréassian, V.: Improvement of a parsimonious model for
594 streamflow simulation, *Journal of Hydrology*, 279, 275–289, [https://doi.org/10.1016/S0022-](https://doi.org/10.1016/S0022-1694(03)00225-7)
595 [1694\(03\)00225-7](https://doi.org/10.1016/S0022-1694(03)00225-7), 2003.
596
597 Piedallu, C., Gégout, J.-C., Perez, V., and Lebourgeois, F.: Soil water balance performs better
598 than climatic water variables in tree species distribution modelling: Soil water balance improves
599 tree species distribution models, *Global Ecology and Biogeography*, 22, 470–482,
600 <https://doi.org/10.1111/geb.12012>, 2013.
601
602 Quintana-Seguí, P., Le Moigne, P., Durand, Y., Martin, E., Habets, F., Baillon, M., Canellas, C.,
603 Franchisteguy, L., and Morel, S.: Analysis of Near-Surface Atmospheric Variables: Validation of
604 the SAFRAN Analysis over France, 47, 92–107, <https://doi.org/10.1175/2007JAMC1636.1>,
605 2008.
606
607 Quintana-Seguí, P., Turco, M., Herrera, S., and Miguez-Macho, G.: Validation of a new
608 SAFRAN-based gridded precipitation product for Spain and comparisons to Spain02 and ERA-
609 Interim, *Hydrol. Earth Syst. Sci.*, 21, 2187–2201, <https://doi.org/10.5194/hess-21-2187-2017>,
610 2017.
611
612 Quintana-Seguí, P., Barella-Ortiz, A., Regueiro-Sanfiz, S., and Miguez-Macho, G.: The Utility of
613 Land-Surface Model Simulations to Provide Drought Information in a Water Management
614 Context Using Global and Local Forcing Datasets, *Water Resour Manage*,
615 <https://doi.org/10.1007/s11269-018-2160-9>, 2019.
616
617 Raymond, F., Ullmann, A., Trambly, Y., Drobinski, P., and Camberlin, P.: Evolution of
618 Mediterranean extreme dry spells during the wet season under climate change, *Reg Environ*
619 *Change*, 19, 2339–2351, <https://doi.org/10.1007/s10113-019-01526-3>, 2019.
620
621 Reynolds, C. A., Jackson, T. J., and Rawls, W. J.: Estimating soil water-holding capacities by
622 linking the Food and Agriculture Organization Soil map of the world with global pedon
623 databases and continuous pedotransfer functions, *Water Resour. Res.*, 36, 3653–3662,
624 <https://doi.org/10.1029/2000WR900130>, 2000.
625
626 Rodell, M., Houser, P. R., Jambor, U., Gottschalck, J., Mitchell, K., Meng, C.-J., Arsenault, K.,
627 Cosgrove, B., Radakovich, J., Bosilovich, M., Entin, J. K., Walker, J. P., Lohmann, D., and Toll,
628 D.: The Global Land Data Assimilation System, *Bull. Amer. Meteor. Soc.*, 85, 381–394,
629 <https://doi.org/10.1175/BAMS-85-3-381>, 2004.
630
631 Stefan, V.G., Indrio G., Escorihuela M.J., Quintana-Seguí P., and Villar, J.M.: High-Resolution
632 SMAP-Derived Root-Zone Soil Moisture Using an Exponential Filter Model Calibrated per Land
633 Cover Type, *Remote Sensing*, 13(6). <https://doi.org/10.3390/rs13061112>, 2021.

634
635 Stein, L., Clark, M. P., Knoben, W. J. M., Pianosi, F., and Woods, R. A.: How Do Climate and
636 Catchment Attributes Influence Flood Generating Processes? A Large-Sample Study for 671
637 Catchments Across the Contiguous USA, *Water Res*, 57,
638 <https://doi.org/10.1029/2020WR028300>, 2021.
639
640 Trambly, Y., Bouaicha, R., Brocca, L., Dorigo, W., Bouvier, C., Camici, S., and Servat, E.:
641 Estimation of antecedent wetness conditions for flood modelling in northern Morocco, *Hydrol.*
642 *Earth Syst. Sci.*, 16, 4375–4386, <https://doi.org/10.5194/hess-16-4375-2012>, 2012.
643
644 Trambly, Y., Amoussou, E., Dorigo, W., and Mahé, G.: Flood risk under future climate in data
645 sparse regions: Linking extreme value models and flood generating processes, *Journal of*
646 *Hydrology*, 519, 549–558, <https://doi.org/10.1016/j.jhydrol.2014.07.052>, 2014.
647
648 Trambly, Y., Koutroulis, A., Samaniego, L., Vicente-Serrano, S. M., Volaire, F., Boone, A., Le
649 Page, M., Llasat, M. C., Albergel, C., Burak, S., Cailleret, M., Kalin, K. C., Davi, H., Dupuy, J.-L.,
650 Greve, P., Grillakis, M., Hanich, L., Jarlan, L., Martin-StPaul, N., Martínez-Vilalta, J., Mouillot, F.,
651 Pulido-Velazquez, D., Quintana-Seguí, P., Renard, D., Turco, M., Türkeş, M., Trigo, R., Vidal,
652 J.-P., Vilagrosa, A., Zribi, M., and Polcher, J.: Challenges for drought assessment in the
653 Mediterranean region under future climate scenarios, *Earth-Science Reviews*, 210, 103348,
654 <https://doi.org/10.1016/j.earscirev.2020.103348>, 2020.
655
656 Tyrallis, H., Papacharalampous, G., and Langousis, A.: A Brief Review of Random Forests for
657 Water Scientists and Practitioners and Their Recent History in Water Resources, *Water*, 11,
658 910, <https://doi.org/10.3390/w11050910>, 2019.
659
660 Vicente-Serrano, S. M., Lopez-Moreno, J.-I., Beguería, S., Lorenzo-Lacruz, J., Sanchez-
661 Lorenzo, A., García-Ruiz, J. M., Azorin-Molina, C., Morán-Tejeda, E., Revuelto, J., Trigo, R.,
662 Coelho, F., and Espejo, F.: Evidence of increasing drought severity caused by temperature rise
663 in southern Europe, *Environ. Res. Lett.*, 9, 044001, [https://doi.org/10.1088/1748-](https://doi.org/10.1088/1748-9326/9/4/044001)
664 [9326/9/4/044001](https://doi.org/10.1088/1748-9326/9/4/044001), 2014.
665
666 Willgoose, G. and Perera, H.: A simple model of saturation excess runoff generation based on
667 geomorphology, steady state soil moisture, *Water Resour. Res.*, 37, 147–155,
668 <https://doi.org/10.1029/2000WR900265>, 2001.
669
670 Wösten, J. H. M., Lilly, A., Nemes, A., and Le Bas, C.: Development and use of a database of
671 hydraulic properties of European soils, *Geoderma*, 90, 169–185, [https://doi.org/10.1016/S0016-](https://doi.org/10.1016/S0016-7061(98)00132-3)
672 [7061\(98\)00132-3](https://doi.org/10.1016/S0016-7061(98)00132-3), 1999.
673
674 Zhao, B., Dai, Q., Han, D., Dai, H., Mao, J., Zhuo, L., and Rong, G.: Estimation of soil moisture
675 using modified antecedent precipitation index with application in landslide predictions,
676 *Landslides*, 16, 2381–2393, <https://doi.org/10.1007/s10346-019-01255-y>, 2019.
677
678
679
680
681
682

683
684
685

686 **TABLE**

687

688 Table 1: Contingency table of the comparison between forecasts and observations or
 689 any two analyses. The symbols a–d are the different numbers of cases observed to
 690 occur in each category.
 691

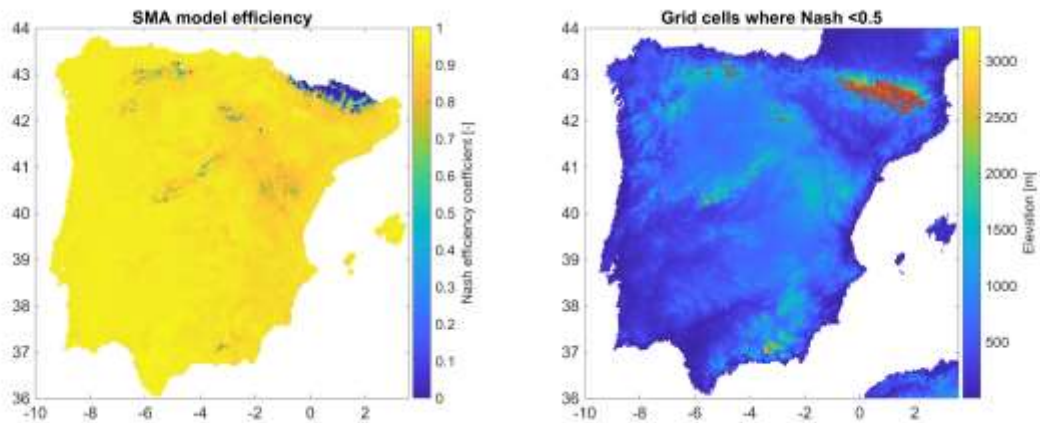
	Observations	
Forecast	1	0
1	a (hit)	b (false alarm)
0	c (miss)	d (correct rejection)

692

693 **FIGURES**

694

695



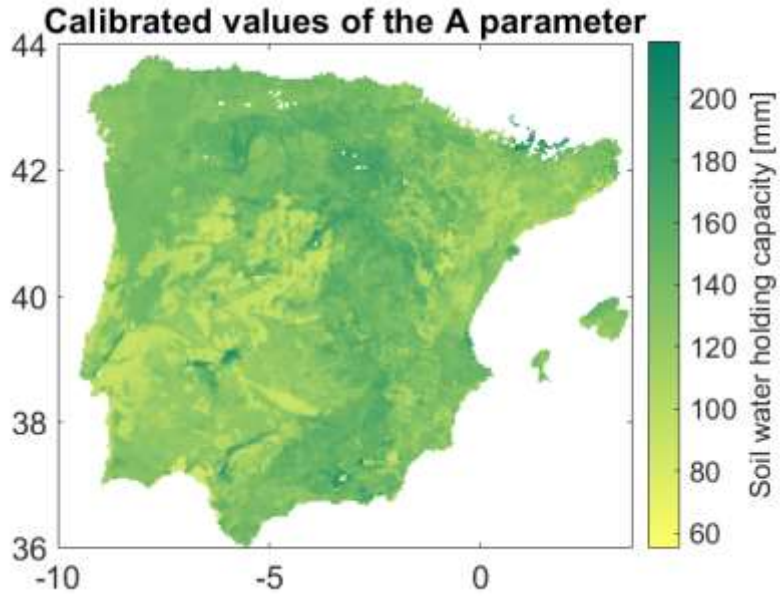
696

697 Figure 1: Efficiency of the SMA model to reproduce soil moisture from SURFEX

698

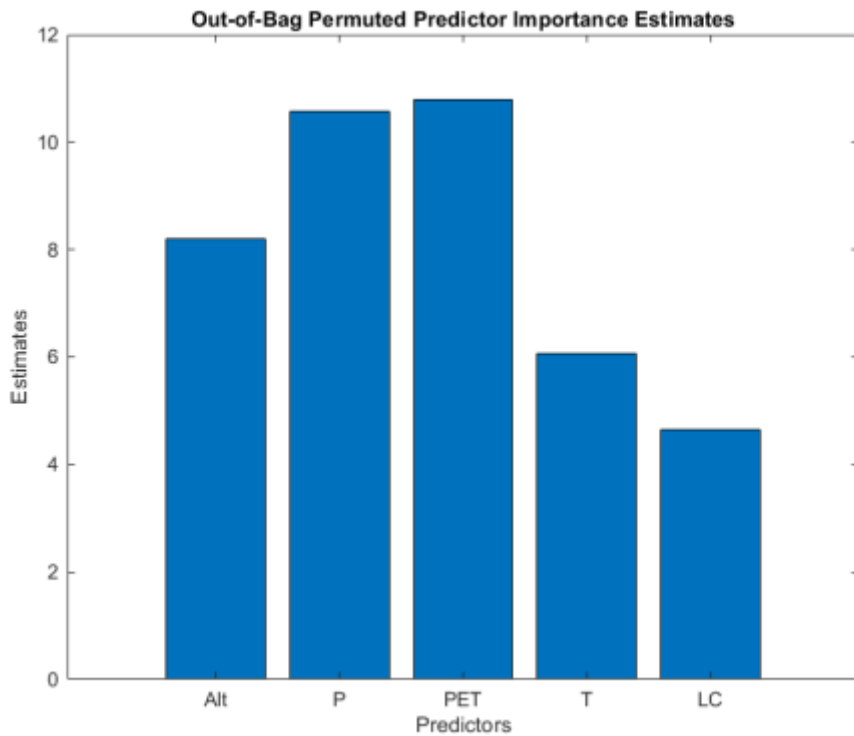
699

700



701
702
703
704

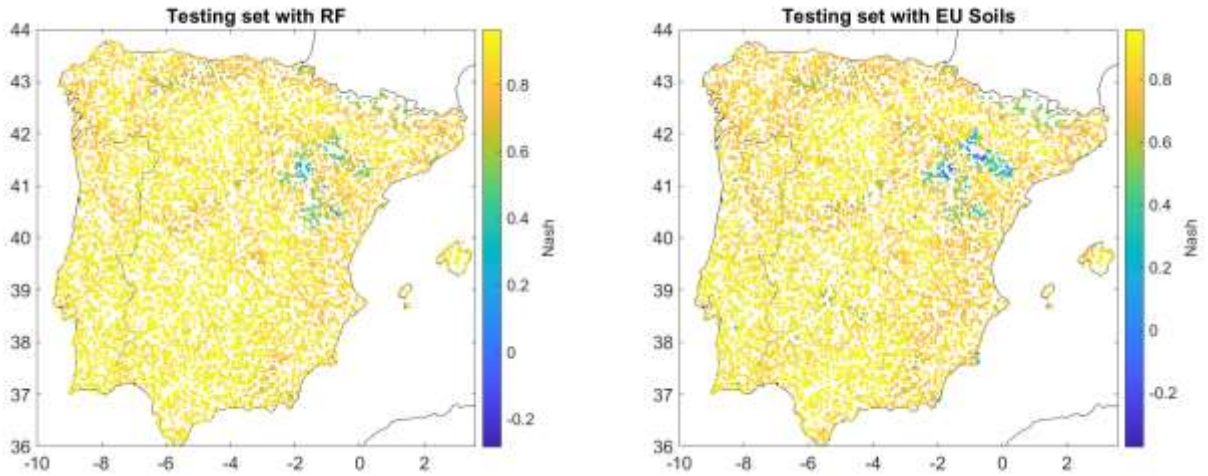
Figure 2: Map of the calibrated values of the A parameter of the SMA model



705
706
707
708
709

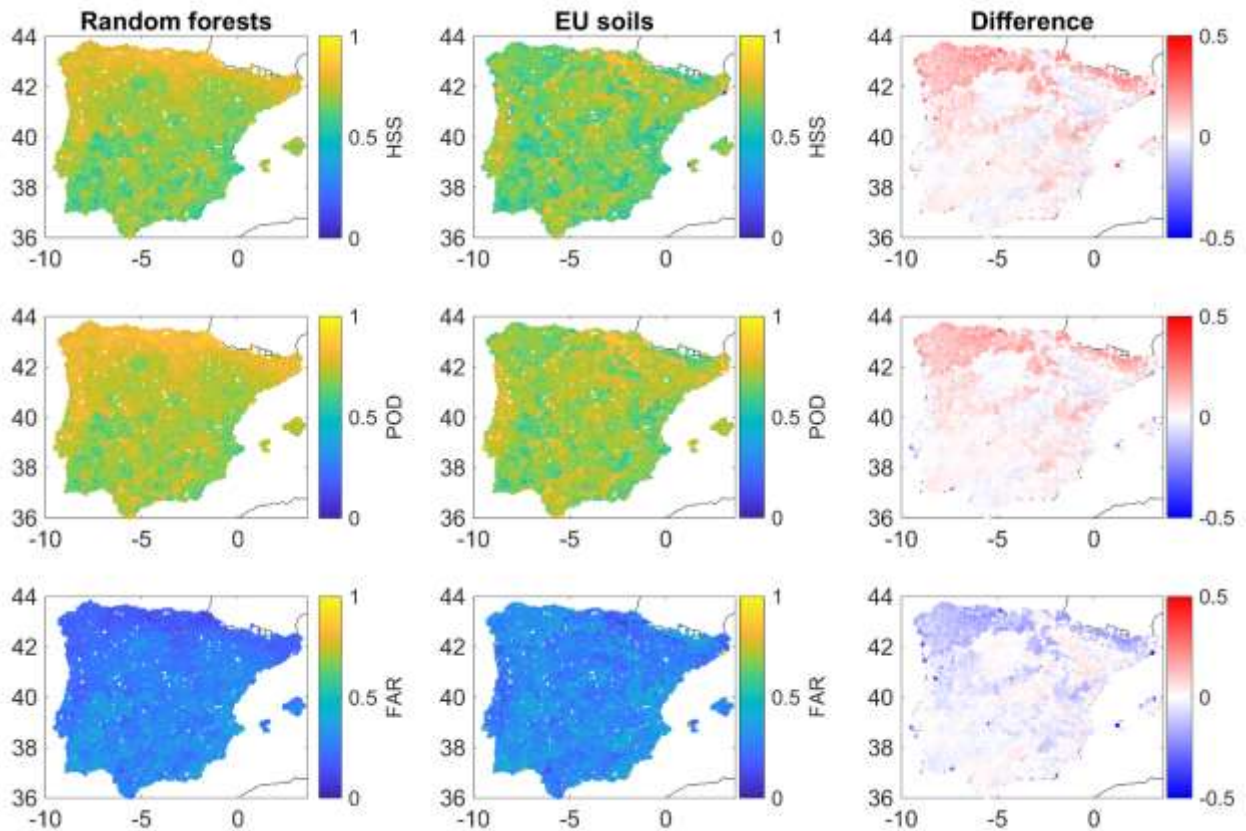
Figure 3: Relative importance of each predictor (Alt= altitude, P= precipitation, PET= potential evapotranspiration, T=temperature, LC=land cover classes) in the Random Forest method

710
711



712
713
714
715
716

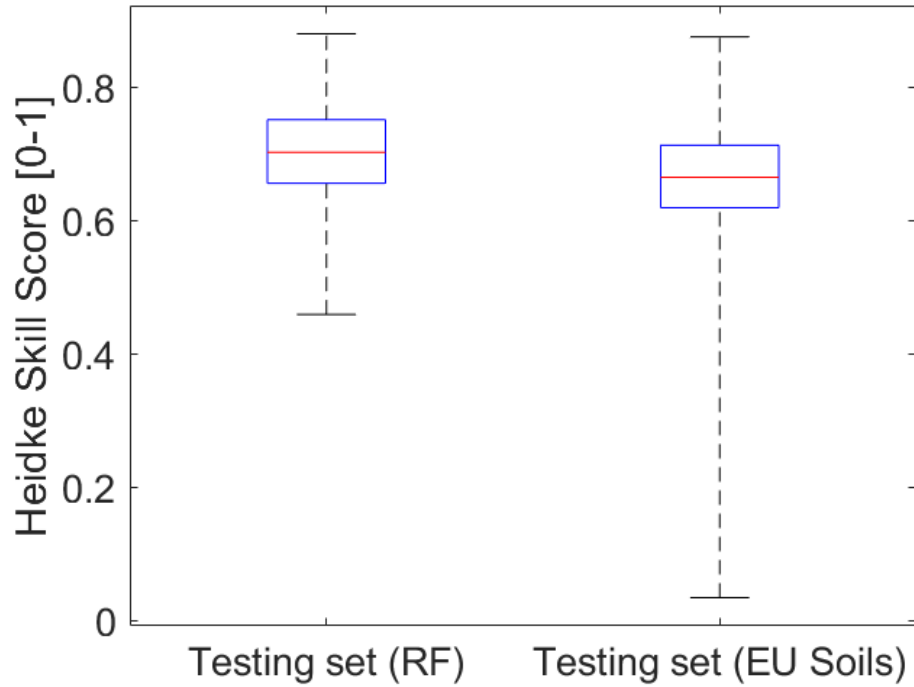
Figure 4: Nash efficiency coefficient obtained for the testing set, with the A parameter of the SMA model estimated by RF (left) or ESDB (right)



717
718
719
720

Figure 5: Validation results in terms of HSS, POD and FAR with A estimated with either Random Forests or European soil database.

721
722
723



724
725
726
727
728
729
730
731
732
733
734
735

Figure 6: Boxplot of the HSS obtained with RF or EU soil maps. The limits of the box represent the 25th and 75 percentiles, the line in the middle refers to the median, and the limits of the whiskers extend to the minimum and maximum values.